Bioorganic & Medicinal Chemistry 18 (2010) 7826–7835

Contents lists available at ScienceDirect

Bioorganic & Medicinal Chemistry

journal homepage: www.elsevier.com/locate/bmc

Studies toward the structural optimization of novel thiazolylhydrazone-based potent antitrypanosomal agents

Marcelo Zaldini Hernandes [a], Marcelo Montenegro Rabello [a], Ana Cristina Lima Leite [a,*], Marcos Veríssimo Oliveira Cardoso [a], Diogo Rodrigo Magalhaes Moreira [a], Dalci José Brondani [a], Carlos Alberto Simone [b], Luiza Campos Reis [c], Marina Assis Souza [c], Valéria Rego Alves Pereira [c], Rafaela Salgado Ferreira [d], James Hobson McKerrow [d]

[a] Department of Pharmaceutical Sciences, Centre for Health Science, Federal University of Pernambuco, 50740-520 Recife, PE, Brazil
[b] Department of Physics and Informatics, Institute of Physics, University of São Paulo, 13560-970 São Carlos, SP, Brazil
[c] Department of Immunology, Aggeu Magalhães Center for Research, Oswaldo Cruz Foundation, 50670-420 Recife, PE, Brazil
[d] Sandler Center for Drug Discovery in Parasitic Diseases, University of California, QB3 1700 4th St, 94158 San Francisco, CA, USA

ARTICLE INFO

Article history:
Received 18 June 2010
Revised 16 September 2010
Accepted 22 September 2010
Available online 29 September 2010

Keywords:
Bioisosterism
Cysteine protease cruzain
Hydrazones
Molecular docking
Thiazoles
Thiosemicarbazones
Trypanosoma cruzi

ABSTRACT

In previous studies, we identified promising anti-*Trypanosoma cruzi* cruzain inhibitors based on thiazolylhydrazones. To optimize this series, a number of medicinal chemistry directions were explored and new thiazolylhydrazones and thiosemicarbazones were thus synthesized. Potent cruzain inhibitors were identified, such as thiazolylhydrazones **3b** and **3j**, which exhibited IC_{50} of 200–400 nM. Furthermore, molecular docking studies showed concordance with experimentally derived structure–activity relationships (SAR) data. In the course of this work, lead compounds exhibiting in vitro activity against both the epimastigote and trypomastigote forms of *T. cruzi* were identified and in vivo general toxicity analysis was subsequently performed. Novel SAR were documented, including the importance of the thiocarbonyl carbon attached to the thiazolyl ring and the direct comparison between thiosemicarbazones and thiazolylhydrazones.

1. Introduction

Chagas' disease, caused by the protozoan parasite *Trypanosoma cruzi* (*T. cruzi*), affects millions of people in Latin American and results in significant mortality, with devastating social and economic consequences. Even though public health programs and vector elimination have decreased the incidence of new infections, Chagas' disease is still endemic in many areas.[1] Additionally, the drug available to treat it (Benznidazole) is decades-old and limited in efficacy, and is plagued by significant side effects and impractical dosing regimens. Therefore, there is an urgent need for new, effectives and safer drugs for treatment of Chagas' disease.[2]

The discovery of enzymes implicated in pathogenesis and host cell invasion of *T. cruzi* has allowed the application of target-based drug design efforts.[3] Given the key role they play at various stages in the life cycle of the parasite and the lack of redundancy of these enzymes compared with the homologous human enzymes, the cysteine protease cruzain,[4] trypanothione reductase,[5] and *trans*-sialidase[6] of *T. cruzi* have thereby emerged as promising drug targets. Cruzain is essential for intracellular replication and differentiation, and is thus involved in all stages of the parasite's life cycle.[7] This enzyme also contributes to immune evasion, hydrolysis of host proteins and cellular invasion in parasites.[8] High-affinity peptidomimetic cruzain inhibitors have been shown to cure *T. cruzi* infection in an immunodeficient-mouse model of infection even in the absence of a functioning adaptive immune response,[9] indicating that this enzyme offers a scientific rationale for (druggable) chemical intervention.[10]

A number of structurally diverse cruzain inhibitors have been reported. Recently, an especial emphasis has been applied to identify nonpeptidic inhibitors (Fig. 1). Based on the known bioisosteric relation between peptide bonds and ureas, the first nonpeptidic cruzain inhibitors identified were aryl ureas and thioureas, which displayed moderate affinity against cruzain and antiproliferative activity against amastigote cell cultures.[11] Following these findings, thiosemicarbazones and their pyrazoline-1-thiocarboxiamide bioisosteres were explored as potential cruzain inhibitors,[12,13] since thioureas and thiosemicarbazones are classically deemed as bioisosteres. This approach yielded highly effective agents against both the enzyme and parasite cell cultures. Inspired by the potency

* Corresponding author. Tel.: +55 81 2126 8511; fax: (+55) 81 2126 8510.
E-mail address: ana.leite@pq.cnpq.br (A.C.L. Leite).

0968-0896/$ - see front matter © 2010 Elsevier Ltd. All rights reserved.
doi:10.1016/j.bmc.2010.09.056

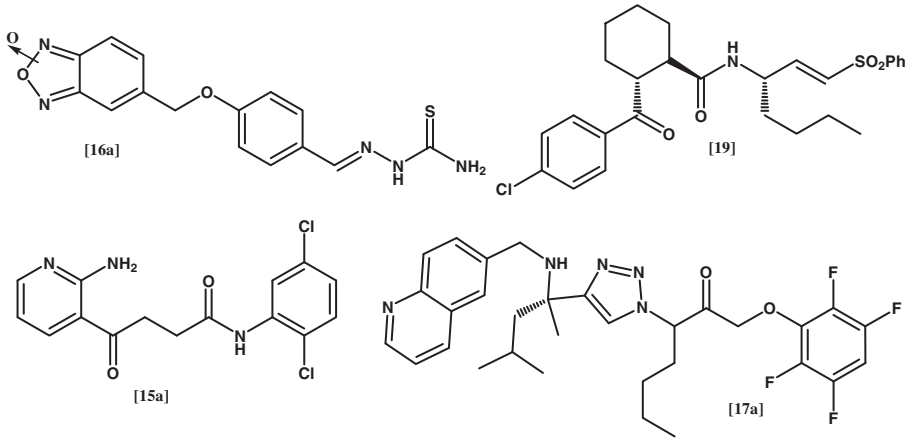

Figure 1. Representative examples of nonpeptidic cruzain inhibitors.

of thiosemicarbazones,[14] other classes of nonpeptidic cruzain inhibitors have been developed, exploring functionalized amides,[15] hydrazones,[16] triazoles/triazines,[17] *N*-acylhydrazones,[18] vinylsulfones,[19] and chalcones[20] as structural prototypes.

Our group has previously described the design and anti-*T. cruzi* screening of a series of *N*-acylthiosemicarbazides and their *N*-acylhydrazide-4-thiazolidone bioisosteres.[21] In our first attempt, the *N*-acyl-4-thiazolidones showed only moderate activity against both trypomastigote and epimastigote forms of the parasite, while *N*-acyl-thiosemicarbazones were inactive.[21] Later, we opted for the structural replacement of the aryl instead of the acyl group in the 4-thiazolidone subunit, and this molecular modification yielded a new congenere series of thiazolylhydrazones.[22] The most potent compound in this series inhibited epimastigote replication (IC_{50} = 0.3 μM) exhibited greater potency when compared with Benznidazole (IC_{50} = 1.8 μM). In silico studies for theses thiazolylhydrazones suggested cruzain was the drug molecular target. Unfortunately, all of our most potent anti-*T. cruzi* agents displayed only low potency when assayed against trypomastigotes (bloodstream form)[22] and subsequently failed when assayed in an in vivo model of acute infection (M. B. P. Soares, D. R. M. Moreira, A. C. L. Leite, unpublished data). Ruthenium complexes with a selected number of these thiazolylhydrazones were also prepared by us. While improved potency against the parasite was noted when compared to their Ru-free thiazolylhydrazones counterparts, undesirable mammal toxicity was observed.[23]

In light of these findings, we turned our attention towards the structural optimization and further identification of improved anti-*T. cruzi* thiosemicarbazones and thiazolylhydrazones. Inspection of the structural features of the most potent anti-*T. cruzi* agents previously identified were used to guide the design of the inhibitors reported here. A number of medicinal chemistry directions were also explored, such as the bioisosterism and conformational restriction.[24] For example, to confirm the importance of the thiazolyl ring, direct comparison of the biological activity of thiazolylhydrazones and thiosemicarbazones was attempted. In addition, the carbonyl of the heterocyclic ring (**3f** and **3j**) was bioisosterically replaced by thiocarbonyl (**6a** and **6b**), since this modification eventually could result in distinct classes of trypanocidal agents. Variable spacer groups, that is, changing the thioether (**2a**) to ethylenic (**4a**) or ethyl (**4b**) were also investigated, resulting in molecules with different conformational restrictions. Finally, a small set of substituents were examined, enabling us to explore a congenere series of thiazolylhydrazones (Fig. 2). By employing these strategies, we aimed to identify new small nonpeptidic cruzain inhibitors of optimized potency against the parasite.

2. Results

2.1. Synthesis

Aromatic aldehydes were obtained by a mild S-alkylation of the 4-substituted thiophenols using bromoacetals, with subsequent deprotection of diethyl acetals under acid hydrolysis; while aromatic ketones were prepared using choroacetone.[21,26b] These procedures allowed reagents for condensation with thiosemicarbazides to be prepared. Under these same conditions, alkylation of 4-nitrobenzenethiol and of 4-(*N*,*N*-dimethylamino)benzenethiol with bromoacetaldehyde diethyl acetal did not afford the expected alkylated products, and only complex mixtures were recovered. Thiosemicarbazones (**2a–j**, **4a**, **4b**) were synthesized by condensation of aldehydes or ketones with thiosemicarbazide, producing the crystalline products in very good yields with short reaction times.[25] Subsequently, the cyclic products (thiazolylhydrazones **3a**–**j** and **5a**) were synthesized in accordance with a recently reported method,[26] treating the appropriate aromatic thiosemicarbazones (**2a–j, 4a**) with α-bromocarboxylic acids, anhydrous sodium acetate and dry ethanol in reflux (Scheme 1).

Thiazolylhydrazones **3a–j** and **5a** were obtained as single isomers and as racemate. No further effort was made to separate the enantiomers, because a rapid epimerization is expected for asymmetric carbons adjacent to carbonyl carbons. Crystallographic data for the compound **3g** is summarized in Supplementary data. The structure determination of **3g** shows that in the solid state this hydrazone adopts the *E* geometry in relation to the C8═N2 bond (Fig. S1). It is in accordance to the literature.[27]

Finally, Lawesson's reagent[28] was used as the thionation agent to the conversion of carbonyl into thiocarbonyl derivatives (**6a and 6b**) with respective yields of 38 and 34% without optimization (Scheme 2). The chemical structure of these products was established using NMR (^1H, ^{13}C and DEPT), HRMS, IR spectral and elemental analysis (for C, H, N, S).

2.2. Biological evaluation

All compounds were preliminarily screened against purified recombinant cruzain at 100 μM; and the subset of active inhibitors had their IC_{50} determined (Table 1). For comparison, two previously described cruzain inhibitors, structurally-related to the thiazolylhydrazones described here, were prepared and screened against cruzain.[12] These inhibitors are 3′-bromopropiophenonethiosemicarbazone and 3′,4′-dichloroacetophenonethiosemicarbazone, designated here **TCC-01** and **TCC-02**, respectively

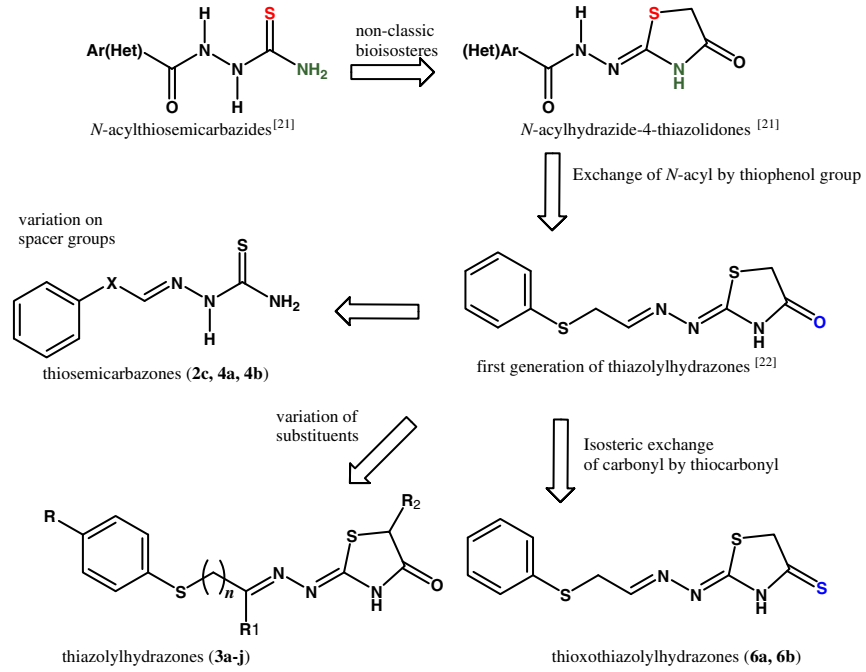

Figure 2. Our design concept for thiosemicarbazones and thiazolylhydrazones as anti-*Trypanosoma cruzi* drug prototypes. This figure also summarizes the molecular optimization strategy developed here.

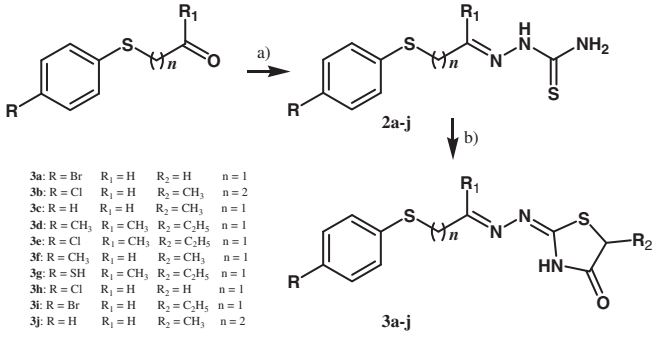

Scheme 1. Synthesis of the thiazolylhydrazones (**3a**–**j**). Reagents and conditions: (a) thiosemicarbazide, H_2O/EtOH, AcOH (three drops), ultrasound irradiation (40 kHz), 60 min; (b) α-bromocarboxylic acids, AcONa, EtOH, reflux, 24 h.

(Fig. 3). Inhibition levels were compared for assays without incubation versus with a 10 min pre-incubation with enzyme. Cruzain inhibition was time-dependent, as expected for covalent inhibitors. To investigate for artifactual promiscuous inhibition by aggregation,[29] enzyme inhibition was compared in presence of 0.01% Triton or in the absence of this detergent.[30] Similar activity was observed in both detergent concentrations, for all active compounds.

The activity of the compounds against *T. cruzi* growth was also determined. To this end, mammal cytotoxicity was firstly evaluated in BALB/c mouse splenocytes and the highest concentration non cytotoxic for the mammalian cells was determined. All compounds were then tested against cultures of the epimastigote and trypomastigote forms of the *T. cruzi* Y strain. Table 2 shows the percentage inhibition at 40 μM and the IC_{50} values, using Benznidazole (**Bdz**) as the reference drug for the cell culture assays. A subset of compounds was tested for time-dependent activity against Y strain epimastigotes. In addition, the in vivo toxicity for selected compounds was measured using female Swiss mice and treated by ip injection with 100 mg kg^{-1} (Table 3).

2.3. Molecular modeling

The optimized structures of compounds **3b**, **3f**, **3j** and **6b** were obtained by application of the RM1[31] method, available as part of the SPARTAN 08' program,[32] using internal default settings for convergence criteria. These new molecules, which had been shown to inhibit cruzain, were synthesized as racemic mixtures, so the molecular modeling treated the two enantiomers (*R* and *S*) independently, and the docking procedure used both isomers for each compound. Docking analysis was carried out on the cruzain binding site (PDB code 1U9Q, available at the RCSB Protein Data Bank, http://www.pdb.org),[33] in which cruzain was co-crystallized in complex with a covalent inhibitor (referred as '186'). The active site was defined as all atoms within a radius of 5.0 Å from the co-crystallized ligand. The GOLD 4.0 program[34] was used for docking calculations.

3. Discussion

The first round of optimization explored various substitution patterns on the aryl and thiazole rings. The compound with a methyl in the R_2 position, **3c**, was inactive against cruzain and parasite cells, while the concomitant insertion of a methyl at the R and R_2 positions led to the discovery of compound **3f**—one of most active cruzain inhibitors and trypanocidal agents. Comparison of *p*-bromophenyl derivatives **3a** and **3i**, revealed that the replacement of hydrogen by the ethyl group at R_2 doubles potency against epimastigote and generates some inhibition against cruzain, although this exchange does not contribute to inhibition of the trypomastigotes. Shortening of the propyl spacer at C1 in compound **3j** to ethyl (compound **3c**) clearly reduces trypanocidal activity and it is deleterious for cruzain affinity.

Next, we exploited the importance of molecular modification of the aryl ring. Compounds **3e** and **3d** inhibited cruzain at similar levels, being weak inhibitors in both cases while compound **3b** was twofold more potent than **3j**. Analyzing the SAR data for these compounds, it can be inferred that the insertion of substituents at

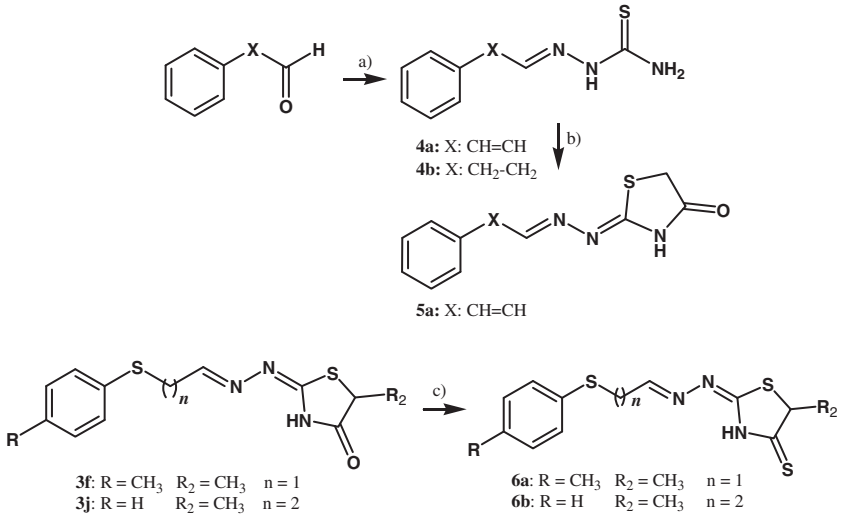

Scheme 2. Top: synthesis of the compounds **4a**, **4b** and **5a**. Bottom: synthesis of 4-thioxothiazolylhydrazones (**6a**, **6b**). Reagents and conditions: (a) thiosemicarbazide, H_2O/EtOH, AcOH (three drops), ultrasound irradiation (40 kHz), 60 min; (b) α-bromoacetic acid, AcONa, EtOH, reflux, 24 h; (c) Lawesson' reagent, toluene, reflux, 24 h.

Table 1
Inhibition of cruzain by inhibitor compounds

Inhibitors	Inhibition (%) at 100 μM	IC_{50}[a] (μM)
2c	28	ND
3a	8	ND
3b	98	0.2
3c	5	ND
3d	22	ND
3e	31	ND
3f	80	20.4
3g	11	ND
3h	11	ND
3i	38	ND
3j	93	0.4
4a	35	ND
4b	ND	ND
5a	8	ND
6a	6	ND
6b	92	0.06
TCC-01	92	0.04
TCC-02	96	0.1

[a] Calculated from ten compound concentrations in duplicates.
ND = not determined.

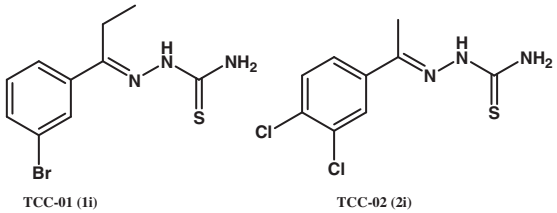

Figure 3. Chemical structures of cruzain ligands previously described as potent cruzain inhibitors. Codes in parenthesis are the same as the original reference.[12]

the *p*-position on the aromatic ring does not significantly contribute to improving the potency for this class of compounds. In addition, for the first round of optimization it was observed that, in general, attaching substituents at the R_1 position in congenere series **3a–j** does not contribute to trypanocidal activity.

Based on their anti-parasitic activity, the most active compounds for series **3a–j** were the derivatives **3f** and **3j**, which exhibited potency similar to that of **Bdz**. For both compounds, efficacy against the parasite was remarkably higher when compared with the thiazolylhydrazones previously described by us.[22] Compound **3j** inhibited the protease with affinity similar to that of **TCC-1**,[12] which constitutes one the most potent previously described cruzain inhibitors. It is worthwhile remarking that compound **3j** was able to reduce the number of parasites at different points in time after treatment, as summarized in Table 3, and that its efficacy was very similar when compared with Benznidazole (**Bdz**).

The second round of optimization explored the bioisosteric relationship within thiosemicarbazones and thiazolylhydrazones. Clearly, thiosemicarbazones **2c**, **4a** and **4b** are antitrypanosomal agents more potent than the correspondent thiazolylhydrazones. For example, the thiosemicarbazone **2c** is ten times more potent than thiazolylhydrazone **3c** against epimastigotes. These results indicate that the thioamide subunit represents a pharmacophoric point for assessment of antitrypanosomal activity. However, the undesired cytotoxicity of thiosemicarbazones was observed when using spleen cell cultures, while the thiazolylhydrazones **3a–j** did not display cytotoxicity at high concentrations (100 μg mL^{-1}).

It was also possible to investigate the effect of molecular flexibility on anti-parasitic activity by comparing compounds **2c** and **4a** or **3c** and **5a**. The replacement of thioether (**2c**) by ethylenic (**4a**) enhanced the potency, but compound **4a** loses selectivity over parasite. It would thus seem that restricted flexibility has an impact on trypanocidal activity. Although both compounds appear to possess very similar geometric conformations, replacing the thioether (**2c**) with ethyl (**4b**) increases potency against the parasite.

The third round of optimization explored bioisosterism.[24a] Replacing the carbonyl group (**3f** and **3j**) with a thiocarbonyl group (**6a** and **6b**) respectively resulted in a 20- and 5-fold increase in potency against the trypomastigote form. From **3j** to **6b** a sevenfold improvement in potency against cruzain was also noted. However, improved antitrypanosomal activity for thioxothiazolylhydrazones **6a** and **6b** was accompanied by cytotoxic properties for mammalian cells at concentrations of lower of than 1.0 μg mL^{-1}. This cytotoxicity is not necessarily inconsistent with the molecular modification performed and may, in part, be responsible for the action against other nonspecific intracellular targets, because thiocarbonyl carbon is more reactive and more likely to react as nucleophilic species than carbonyl carbon.

To confirm the in vitro cytotoxicity observed for **6a** and **6b**, the general toxicity in mice was assessed (Table 3). In this short assay, **6a** and **6b** were toxic at single dose of 100 mg kg^{-1} weight, while at the same dose **6b** bioisosters (i.e., **3j**) was not (with 100% survival

Table 2
Evaluation of efficacy and cytotoxicity of inhibitors in cell culture

Compd	Epimastigotes after 11 days		Trypomastigotes after 24 h IC_{50}[b] (μM)	BALB/c cytotoxicity[c] in μg mL^{-1}
	Inhibition[a] (%)	IC_{50}[b] (μM)		
2c	100	13.4	158	5 (22 μM)
3a	31.5	42.9	ND	>100
3b	10	32.1	ND	>100
3c	4.0	166.9	44.2	>100
3d	40	45.1	76.9	>100
3e	24	62.9	148.1	>100
3f	97	6.7	84.8	>100
3g	41	40.8	54.6	>100
3h	8.0	43.9	82.4	>100
3i	77	26.9	ND	>100
3j	100	2.9	10.0	>100
4a	99	7.3	7.4	<1.0
4b	ND	3.7	3.7	<1.0
5a	ND	2.3	10.1	<1.0
6a	ND	6.1	4.5	<1.0
6b	ND	8.1	2.3	1.0
TCC-01	ND	15.4	11.1	1.0 (3.6 μM)
TCC-02	ND	8.5	39.5	1.0 (3.8 μM)
Bdz	97	6.6	5.0	25

ND is not determined at tested concentrations. Bdz is Benznidazole, the reference drug.
[a] Percent growth inhibition determined for each compound at 40 μM.
[b] Calculated from six concentrations using data obtained from at least three independent experiments. S.D. less than 10%.
[c] Expressed as the highest concentration tested that was not cytotoxic for BALB/c mouse splenocytes. In parenthesis, values are quoted in micromolar.

Table 3
Time-dependent growth inhibition of the Y strain *T. cruzi* and animal toxicity for the most active compounds

Compd	Inhibition (%) against epimastigote[a]		In vivo toxicity[b] (n = 6 per treatment)
	15 h	7 days	
2c	NT	NT	4/(√)
3f	85	97	NT
3i	0	61	6/(√)
3j	75	100	6/(√)
6b	NT	94	0/(√)
Bdz	43	85	NT

[a] Percent growth inhibition determined for each compound at 40 μM.
[b] Number of animals survive after ip treatment (at single dose of 100 mg kg^{-1} weight). The control group received only solvent and no deaths were observed. NT = not tested.

of animals). Relevant SAR emerges from these data. The trypanocidal activity was quite different between the sub-series: thioxothiazolylhydrazones (**6a, 6b**), thiosemicarbazones (**2c, 4a, 4b**), and thiazolylhydrazones (**3a–j**). Both thioxothiazolylhydrazones and thiosemicarbazones showed higher mammal cytotoxicity than thiazolylhydrazones. This suggests that the presence of a thiocarbonyl group contributes to unspecific cytotoxicity in both parasite and mammalian cells (Fig. 4). Therefore, an important contribution from this study is to show for the first time that the bioisosteric relation between thiosemicarbazones, thiazolylhydrazones, and thioxothiazolylhydrazones clearly produce distinct bioactive compounds. Du and co-workers[12] have observed that the bioisosteres thiosemicarbazones and pyrazoline-1-thiocarboxamide also are distinct regarding cruzain inhibition.

To illuminate the SAR obtained against cruzain, these compounds were investigated by molecular docking. The proposed binding mode for these ligands was determined as the highest (most positive) score among the possible solutions for each ligand generated according to the GoldScore Fitness Function. Figure 5 shows the superimposition of the best docking solutions for compounds **3b**, **3f**, **3j** and **6b** and the crystallographic structure of the '186' co-crystallized ligand. Furthermore, Fig. 6 illustrates the trend observed between the in silico docking scores and the in vitro pIC_{50} data, which indicates that the most potent molecules, or the compounds with the higher values for pIC_{50} (equals $-\log IC_{50}$ for cruzain inhibition, in molar concentration), are those ones with the higher docking scores, demonstrating that the molecules with more stable or positive docking scores (*i.e.*, greater in silico affinity to cruzain) are also the most potent cruzain inhibitors. Only the new molecules **3b**, **3f**, **3j** and **6b**, with known IC_{50} values for cruzain inhibition (see Table 1) were used, in order to allow a comparative discussion. Moreover, it should also be pointed out that while the (*R*) enantiomer for molecule **6b** seems to be the most potent in silico, in the case of molecule **3b**, the (*S*) isomer seems to have higher affinity for the target, in comparison with the opposite enantiomer. After a detailed comparative

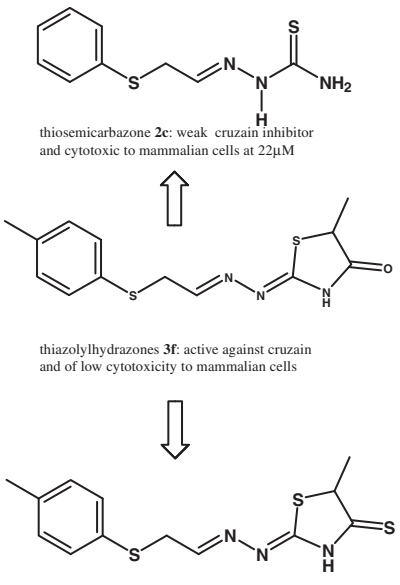

Figure 4. Summary of important SAR.

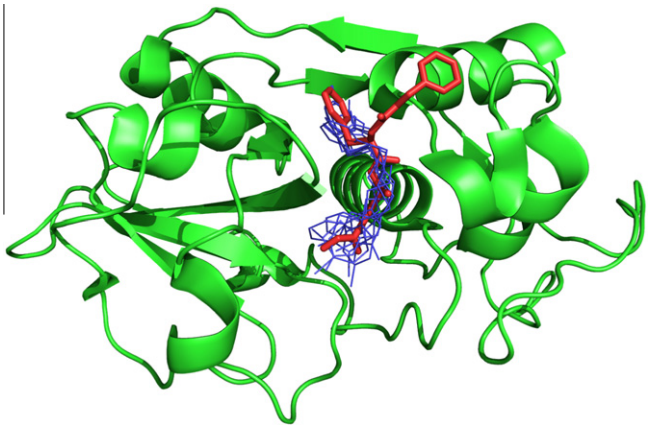

Figure 5. Superimposition of the best docking solutions for the (*R*) and (*S*) enantiomers of the compounds **3b**, **3f**, **3j** and **6b** (wireframe model) and the co-crystallized ligand '186' (stick model) in PDB structure 1U9Q of cruzain (ribbons model). Figure generated with Pymol.[35]

analysis of the docking results between the enantiomers for each molecule, it seems that while the (*R*) isomers occupies the binding site of cruzain with the thiazolylhydrazone portion of the molecule oriented toward the Cys-25 residue, the (*S*) enantiomer is positioned in an opposite way, with the thiazolylhydrazone moiety oriented to the Gly-66 side. Therefore, these differences in ligand position depending upon the chirality of the compounds seem to affect the binding affinity of molecules **6b** and **3b** in an opposite manner, for example.

The molecular interactions for these compounds in the binding mode predicted by docking were compared to the ones previously observed in ligands co-crystallized with cruzain. For illustration, we compare the inhibitor **6b*R*** and the co-crystallized ligand '186'. According to the docking prediction, ligand **6b*R*** hydrogen bonds to the Gln-19, Cys-25 and Trp-177 residues (Fig. 7, Table 4). The co-crystallized ligand '186' also forms hydrogen bonds (HB) with the Gln-19 residue, but this ligand also interacts with Gly-66 and Asp-158 residues. A detailed mapping of the most important intermolecular interactions between cruzain and molecules **3f*R***, **6b*R*** and '186' can be found in Table 4, with hydrophobic and hydrophilic (hydrogen bond) contributions. The molecule **3f*R*** was included in this analysis because it has an inhibitory potency more than 300 times lower in comparison with **6b*R***, and the reason for this result, in the molecular level, seems to be two additional strong hydrogen bonding interactions that **6b*R*** establishes with Gln-19 and Trp-177 residues.

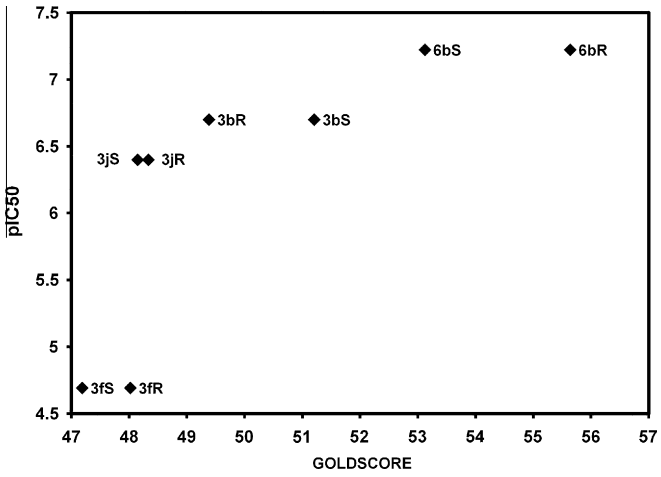

Figure 6. Trend between the GOLD docking score and the pIC_{50} (equals $-\log IC_{50}$ for cruzain inhibition, in molar concentration) values for **3b**, **3f**, **3j** and **6b**. The (*S*) and the (*R*) symbols stand for the respective enantiomers.

4. Conclusions

This paper describes optimization of antitrypanosomal properties of a family of thiazolylhydrazones. As a result of our efforts, new potent cruzain inhibitors and *T. cruzi* growth inhibitors were identified, such as thiazolylhydrazones **3b** and **3j**. Compound **3j** exhibits at least 30-fold selectivity to parasites versus mammalian cells, meriting further evaluation in animal model. Furthermore, our docking results (GOLD scores) show a trend that is consistent with the in vitro data (pIC_{50}), revealing the reliability of the theoretical models applied here. The binding patterns observed for all docked molecules, particularly for **3b**, **3f**, **3j** and **6b**, are quite similar to those of the '186' co-crystallized inhibitor, showing important hydrogen bonds with the same residues on the active site. Thus, insights gained from this present study could be useful for subsequent design of cruzain and anti-*T. cruzi* inhibitors.

5. Experimental section

5.1. Chemistry

All common laboratory chemicals were purchased from commercial sources and used without further purification. Melting points were determined using a Thomas Hoover apparatus and are uncorrected. FTIR spectra were obtained using KBr pellets. ^{1}H NMR, ^{13}C NMR and DEPT spectra were measured on a Varian UNITYplus-300 NMR spectrometer (at 300 MHz for ^{1}H and 75.5 MHz for ^{13}C) using DMSO-d_6 or D_2O as solvents and TMS as an internal standard. Coupling constants (*J*) are given in hertz. Microanalysis (C, H, N, S) of the new compounds was performed on Carlo Erba instrument model E-1110 and results agreed with the theoretical values within (0.4%). High-resolution mass spectra (electrospray ionization) were recorded at IP-TOF equipment (Shimatzu). Thin-layer chromatography (TLC) was carried out on silica gel plates with a fluorescence indicator of F_{254} (0.2 mm, E. Merck); the spots were visualized in UV light, whilst, for compounds **2c**, **4b**, **5a**, the plates were exposed in a chamber containing iodine vapor which revealed the spots. Column chromatography was performed on silica using Kiesegel 60 (230–400 mesh, E. Merck). The obtained spectral of ^{1}H NMR and elemental analysis of **TCC-01** and **TCC-02** were in agreement with the reported data[12] and their original codes are **1i** and **2i**, respectively.

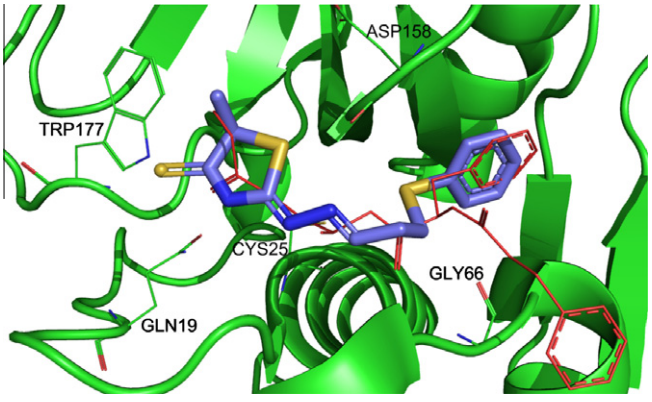

Figure 7. Detailed view of the docking solution for the (*R*) enantiomer of the molecule **6b** (stick model) in comparison with the position of the '186' co-crystallized ligand (wireframe model). The most important residues involved in specific interactions (hydrogen bonds) are labeled. Figure generated with Pymol.[35]

Table 4
Details of the intermolecular interactions of compounds **3f*R*** and **6b*R*** with cruzain, in comparison with the '186' co-crystallized ligand

Cruzain residues	Ligands and intermolecular interactions with cruzain[a,b]					
	'186'		**3f*R***		**6b*R***	
	HB	HP	HB	HP	HB	HP
Gln-19	2.84	—	—	—	2.49	—
Cys-25	—	Yes	3.24	—	3.21	—
Gly-65	—	Yes	—	—	—	—
Gly-66	3.05	Yes	—	—	—	—
Leu-67	—	Yes	—	Yes	—	Yes
Met-68	—	Yes	—	Yes	—	Yes
Ala-133	—	Yes	—	Yes	—	Yes
Leu-157	—	Yes	—	Yes	—	Yes
Asp-158	3.12	Yes	—	—	—	—
His-159	—	Yes	—	—	—	—
Trp-177	—	—	—	—	3.28	—

[a] HB stands for hydrogen bonds and HP for hydrophobic interactions, respectively.
[b] All distance values are given in Å.

5.1.1. Starting materials

The corresponding diethyl acetals or ketones were prepared according to reference [21], while subsequently deprotection of acetals to aldehydes was performed using classical acid hydrolysis. Thiosemicarbazones **2c**, **4a** and **4b** were obtained by reaction of aromatic aldehydes (1.0 mmol) with thiosemicarbazide (1.2 mmol) in acid medium (20 mL of EtOH and five drops of glacial acetic acid).[26] The mixture was then maintained under sonication (40 kHz) for 60 min. leading to the end of the reaction a powder solid that was filtered and washed with diethyl ether. Purification was carried out by way of recrystallization using absolute ethanol or water/ethanol (1:2).

5.1.1.1. N^1-[Phenylthioethylidene]thiosemicarbazide (2c). 80% yield, mp 116–17 °C (from ethanol); lit[26] mp112–113 °C. ^{1}H NMR (DMSO-d_6, 300 MHz) and ^{13}C NMR (DMSO-d_6, 75.5 MHz) spectra agreed with the proposed structure.

5.1.1.2. N^1-[3-(phenyl)propenilidene]thiosemicarbazide (4a). 77% yield, mp 111–112 °C (from ethanol); lit[26] mp 113–115 °C. ^{1}H NMR (DMSO-d_6, 300 MHz) and ^{13}C NMR (DMSO-d_6, 75.5 MHz) spectra agreed with the proposed structure.

5.1.1.3. N^1-[3-(Phenyl)propylide-2-ene]thiosemicarbazide (4b). 62% yield, mp 101 °C (from ethanol); ^{1}H NMR (DMSO-d_6, 300 MHz): δ 2.5 (m, 2H, CH_2); 2.5 (dt, J = 10 and J = 17 Hz, 2H, CH_2); 7.11 (t, J = 17 Hz, 1H, CH=N); 7.18–7.23 (m, 6H, 5H for Ar and 1H for NH_2); 8.32 (s, 1H, NH_2); 10.23 (s, 1H, NH). ^{13}C NMR (DMSO-d_6, 75.5 MHz): δ 31.7 (CH_2), 40.3 (CH_2, near of DMSO′ signal), 130.5 (Ar); 132.4 (Ar); 135.3 (Ar); 137.0 (Ar); 147.9 (CH=N); 173.4 (C=S). IR (KBr, cm^{-1}) ν 3411 (NH_2). 3297 (NH); 1677 (C=N). Anal. Calcd for $C_{10}H_{13}N_3S$: C, 57.94; H, 6.32; N, 20.27; S, 15.47. Found: C, 57.81; H, 6.48; N, 20.34; S, 15.37.

5.1.2. General procedure for the synthesis of compounds 3a–j and 5a

A solution of arylthiosemicarbazone (2 mmol) in EtOH (20 mL) was added to a suspension of anhydrous AcONa (2.2 mmol) in 10 mL of EtOH and stirred for 15 min. Subsequently, α-bromocarboxylic acid (3.0 mmol) was added at room temperature and the reaction stirred on reflux for 24 h. After this time, the solvent was completely removed and ice was added. The precipitate formed was filtered and washed with 0.1 M of $KHSO_4$ and water. The impure product was recrystallized in absolute ethanol to obtain the compounds in 42–70% yields.

5.1.2.1. 2-[(*p*-Bromophenyl)thioethylidenehydrazinyl] thiazolidin-4-one (3a)[23]. 56% yield, mp 116–17 °C (from water); lit[26] mp 115–116 °C. ^{1}H NMR (DMSO-d_6, 300 MHz) and ^{13}C NMR (DMSO-d_6, 75.5 MHz) spectra agreed with the proposed structure.

5.1.2.2. 2-[(*p* -Chlorophenylthio)propylide-1-enehydrazinyl]-5-methylthiazolidin-4-one (3b). 53% yield, mp 128 °C (from ethanol); ^{1}H NMR (DMSO-d_6, 300 MHz): δ 1.62 (d, 3H, CH_3); 3.32 (t, J = 8 Hz, 2H, S–CH_2–CH_2); 3.60 (m, 2H, S–CH_2–C=); 3.90 (m, 1H, S–CH); 7.43 (d, 2H, Ar); 7.88 (d, 2H, Ar); 7.90 (t, 1H, CH=N); 9.70 (s, 1H, NH); ^{13}C NMR (DMSO-d_6, 75.5 MHz): δ 17.2 (CH_3), 36.2 (CH_2), 37.1 (CH–S–C=);42.4 (S–CH_2), 44.0 (CH_2–C=), 128.9 (Ar); 129.0 (Ar); 134.5 (Ar), 137.7 (Ar); 139.5 (CH=N); 157.2 (C=N), 173.1 (C=O). IR (KBr, cm^{-1}) ν = 3132 (NH); 1750 (C=O), 1615 and 1596 (C=N).

5.1.2.3. 2-[(phenylthio)ethylidenehydrazinyl] thiazolidin-4-one (3c). 70% yield, mp 131 °C (from ethanol); ^{1}H NMR (DMSO-d_6, 300 MHz): δ 3.72 (d, 2H, J = 5 Hz, S–CH_2–CH=); 3.95 (s, 2H, S–CH_2–C=O); 7.20–7.43 (m, 5H, Ar); 7.51 (t, 1H, J = 5 Hz, CH=N); 10.96 (br, 1H, NH); ^{13}C NMR (DMSO-d_6, 75.5 MHz): δ 31.2 (S–CH_2–C=), 43.1 (S–CH_2–C=O); 126.3 (Ar); 127.0 (Ar); 128.2 (Ar); 129.8 (Ar); 133.0 (Ar); 146.5 (CH=N); 151.8 (C=N), 175.3 (C=O). IR (KBr, cm^{-1}) ν = 3132 (NH); 1725 (C=O), 1615 and 1596 (C=N), Anal. Calcd for $C_{11}H_{11}N_3OS_2$: C, 49.79; H, 4.18; N, 15.84; S, 24.16. Found: C, 50.03; H, 4.38; N, 15.64; S, 24.26.

5.1.2.4. 2-[(*p* -Methylphenylthio)propylide-2-enehydrazinyl]-5-ethylthiazolidin-4-one (3d). 59% yield, mp 115 °C (from ethanol); ^{1}H NMR (DMSO-d_6, 300 MHz): δ 0.89–0.93 (t, 3H, J = 15 Hz, CH_3); 1.66–1.76 (m, 1H, CH_2–CH_3); 1.88–1.92 (m, 1H, CH_2–CH_3); 2.03 (s, 3H, CH_3); 3.38 (s, 3H, CH_3-Ar); 3.83 (s, 2H, CH_2–S); 4.11–4.15 (m, 1H, CH), 7.34 (m, 2H, Ar) 7.40 (m, 2H, Ar); 11.80 (s, 1H, NH); ^{13}C NMR (DMSO-d_6, 75.5 MHz): δ 10.2 (CH_3), 16.0 (CH_3); 19.7 (CH_3); 25.4 (CH_2), 48.8 (S–CH_2); 128.8 (Ar); 130.3 (Ar); 130.6 (Ar); 134.5 (Ar); 161.4 (C=N); 175.8 (C=O). IR (KBr, cm^{-1}) ν = 3052 (NH); 1722 (C=O), 1634 and 1587 (C=N).

5.1.2.5. 2-[(*p* -Clorophenylthio)propylide-2-enehydrazinyl]-5-ethylthiazolidin-4-one (3e). 62% yield, mp 140 °C (from ethanol); ^{1}H NMR (DMSO-d_6, 300 MHz): δ 0.93–0.98 (t, 3H, J = 15 Hz, CH_3); 1.05–1.16 (m, 1H, CH_2–CH_3); 1.20–1.30 (m, 1H, CH_2–CH_3); 2.13 (s, 3H, CH_3); 3.83 (s, 2H, CH_2–S); 3.91–3.98 (m, 1H, CH), 7.47 (m, 2H, Ar) 7.72 (m, 2H, Ar); 11.10 (s, 1H, NH); ^{13}C NMR (DMSO-d_6, 75.5 MHz): δ 11.2 (CH_3), 15.1 (CH_3); 27.2 (CH_2), 43.0 (S–CH_2); 126.0 (Ar); 128.2 (Ar); 128.8 (Ar); 139.2 (Ar); 140.2

(Ar); 153.4 (C=N); 177.3 (C=O). IR (KBr, cm^{-1}) ν = 3062 (NH); 1725 (C=O), 1630 and 1590 (C=N).

5.1.2.6. 2-[(*p*-Methylphenylthio)ethylidenehydrazinyl]-5-methylthiazolidin-4-one (3f). 49% yield, mp 146 °C (from ethanol); ^{1}H NMR (DMSO-d_6, 300 MHz): δ 1.02–1.10 (m, 3H, CH_3); 3.47 (s, 3H, CH_3); 3.82 (d, 2H, J = 8 Hz, CH_2–S); 4.31–4.39 (m, 1H, CH), 7.29 (m, 2H, Ar) 7.41 (m, 2H, Ar); 7.75 (t, 1H, J = 8 Hz, CH=N); 10.79 (br s, 1H, NH); ^{13}C NMR (DMSO-d_6, 75.5 MHz): δ 14.1 (CH_3), 29.4 (CH_3), 43.4 (CH_2), 48.2 (S–CH_2); 127.3 (Ar); 128.0 (Ar); 134.1 (Ar); 134.8 (Ar); 142.4 (CH=N); 165.2 (C=N); 175.2 (C=O). IR (KBr, cm^{-1}) ν = 3100 (NH); 1725 (C=O), 1670 and 1630 (C=N).

5.1.2.7. 2-[(4-Mercaptophenylthio)propylide-2-enehydrazinyl]-5-ethylthiazolidin-4-one (3g). 62% yield, mp 140–1 °C (from ethanol); ^{1}H NMR (DMSO-d_6, 300 MHz): δ 0.92–0.98 (m, 3H, CH_3); 1.05–1.16 (m, 2H, CH_2–CH_3); 2.07 (s, 4H, CH_3 and SH); 3.92 (s, 2H, CH_2–S); 4.21–4.29 (m, 1H, CH), 7.41–7.61 (m, 4H, Ar); ^{13}C NMR (DMSO-d_6, 75.5 MHz): δ 19.2 (CH_3), 24.4 (CH_3), 42.9 (CH_2), 46.3 (S–CH_2); 129.2 (Ar); 129.9 (Ar); 132.1 (Ar); 132.7 (Ar); 133.9 (Ar); 149.3 (CH=N); 176.1 (C=O). IR (KBr, cm^{-1}) ν = 3090 (NH); 1720 (C=O), 1630 and 1598 (C=N).

5.1.2.8. 2-[(*p* -Chlorophenylthio)ethylidenehydrazinyl]thiazolidin-4-one (3h). 42% yield, mp 148–9 °C (from ethanol); ^{1}H NMR (DMSO-d_6, 300 MHz): δ 3.62 (t, 2H, J = 12 Hz, CH_2–S); 4.02 (s, 2H, CH_2), 7.31 (m, 2H, Ar); 7.61- 7.61 (m, 2H of Ar, 1H of CH=N); 11.9 (s, 1H, NH); ^{13}C NMR (DMSO-d_6, 75.5 MHz): δ 43.2 (CH_2), 44.9 (CH_2-Het); 128.9 (Ar); 130.2 (Ar); 136.4 (Ar); 136.9 (Ar); 144.3 (CH=N); 162.3 (C=N); 178.0 (C=O). IR (KBr, cm^{-1}) ν = 3170 (NH); 1710 (C=O), 1640 and 1608 (C=N).

5.1.2.9. 2-[(*p* -Bromophenylthio)ethylidenehydrazinyl]-5-ethylthiazolidin-4-one (3i). 49% yield, mp 165 °C (from ethanol); ^{1}H NMR (DMSO-d_6, 300 MHz): δ 0.94–1.09 (m, 3H, CH_3); 1.85–1.92 (m, 2H, CH_2–CH_3); 3.52 (t, 2H, J = 12 Hz, CH_2–S); 4.12 (m, 1H, CH_2), 7.39 (m, 2H, Ar); 7.71–7.91 (m, 2H of Ar, 1H of CH=N); 11.3 (s, 1H, NH); ^{13}C NMR (DMSO-d_6, 75.5 MHz): δ 10.9 (CH_3), 24.4 (CH_2), 45.1 (CH_2), 132.1 (Ar); 132.9 (Ar); 139.4 (Ar); 139.9 (Ar); 144.3 (CH=N); 174.0 (C=O). IR (KBr, cm^{-1}) ν = 3170 (NH); 1710 (C=O), 1640 and 1608 (C=N).

5.1.2.10. 2-[(Phenylthio)propylide-1-enehydrazinyl]-5-methylthiazolidin-4-one (3j). 47% yield, mp 140–1 °C (from ethanol); ^{1}H NMR (DMSO-d_6, 300 MHz): δ 1.45–1.56 (m, 3H, CH_3); 3.42 (d, 2H, J = 10 Hz, CH_2–S); 4.22 (m, 1H, CH), 7.35–7.49 (m, 4H, Ar); 7.91 (t, 1H, J = 10 Hz, CH=N); ^{13}C NMR (DMSO-d_6, 75.5 MHz): δ 14.9 (CH_3), 43.2 (CH_2), 44.2 (CH_2), 132.9 (Ar); 134.2 (Ar); 134.8 (Ar); 136.9 (Ar); 146.2 (CH=N); 168.5 (C=N); 174.0 (C=O). IR (KBr, cm^{-1}) ν = 3100 (NH); 1710 (C=O), 1630 and 1600 (C=N).

5.1.2.11. N^1 -[(3-Phenyl)propenilidenehydrazinyl]thiazolidin-4-one (5a). 60% yield, mp 238–9 °C (dec) (from ethanol); ^{1}H NMR (DMSO-d_6, 300 MHz): δ 3.87 (s, 2H, CH_2–S), 7.03–7.19 (m, 2H, CH), 7.31–7.45 (m, 3H, Ar); 7.56–7.73 (d, J = 9 Hz, 2H, CH), 8.16 (d, J = 9 Hz, 1H, CH=N). ^{13}C NMR (DMSO-d_6, 75.5 MHz): δ 33.1 (CH_2–S), 125.3 (CH), 127.3 (CH), 128.9 (Ar), 129.1 (Ar), 135.7 (Ar); 141.2 (Ar); 149.05 (Ar), 158.6 (CH=N), 164.6 (C=N); 174.3 (C=O). IR (KBr, cm^{-1}) ν = 3197 (NH); 1760 (C=O), 1680 and 1607 (C=N).

5.1.3. Conversion of aryl-4-oxothiazolylhydrazones in aryl-4-thioxothiazolylhydrazones (6a and 6b)

The aryl-4-oxothiazolylhydrazone **3f** (1.0 mmol) was suspended in dry toluene (20 mL) containing five drops of DMF and added to a solution of Lawesson' reagent (2.0 mmol) in toluene. The mixture was heated under reflux (110 °C) under dry nitrogen during 24 h (controlled by TLC). After this time, the solvent was evaporated, washed with cold water and filtered off. Due to the close R_f values of unreactant **3f** and product **6a**, the crude mixture was subjected to a first column (to remove impurities) and a further purification using a second silica column (EtOAc/DCM, 9:1 as an eluent) to yield pure **6a** in the form of yellow crystals. Similar procedure was done to compound **6b**.

5.1.3.1. 2-[(*p*-Methylphenylthio)ethylidenehydrazinyl]-5-methylthiazolidine-4-thione (6a). 38% yield, mp 125 °C (from DCM); ^{1}H NMR (DMSO-d_6, 300 MHz): δ 1.67–1.73 (m, 3H, CH_3), 3.21 (s, 3H, CH_3), 3.71 (d, 2H, J = 8 Hz, CH_2–S), 3.94 (m, 1H, CH–S), 7.01 (d, 2H, Ar); 7.20 (d, 2H, Ar); 7.91 (t, J = 8 Hz, 1H, CH=N), 10.09 (s, 1H, NH). ^{13}C NMR (DMSO-d_6, 75.5 MHz): δ 19.3 (CH_3), 24.3 (CH_3), 39.5 (CH–S), 47.7 (CH_2–S), 122.7, 126.3, 128.0, 132.6, 135.7; 141.2; 149.0, 157.6 (CH=N), 169.9 (CH=N); 191.1 (C=S). IR (KBr, cm^{-1}) ν = 3201 (NH); 1602 and 1598 (C=N), 1209 (C=S).

5.1.3.2. 2-[(*p*-Methylphenyl)thiopropylidenehydrazinyl]-5-methylthiazolidine-4-thione (6b). 34% yield, mp 137 °C (from DCM); ^{1}H NMR (DMSO-d_6, 300 MHz): δ 1.47–1.73 (m, 6H, CH_3), 3.48–3.61 (m, 4H, 2CH_2), 3.94 (m, 1H,CH_2–S), 7.35 (m, 4H, Ar); 8.31 (t, J = 11 Hz, 1H, CH=N), 9.49 (s, 1H, NH). ^{13}C NMR (DMSO-d_6, 75.5 MHz): δ 16.3 (CH_3), 18.3 (CH_2), 24.8 (CH_3), 45.31 (CH_2-S), 126.3, 127,3, 128.0, 130.2, 136.0; 145.2; 151.0, 159.2 (CH=N), 170.9 (CH=N); 186.5 (C=S). IR (KBr, cm^{-1}) ν = 3191 (NH); 1672 and 1608 (C=N), 1206 (C=S).

5.2. Pharmacology

5.2.1. Cruzain inhibition assays

Cruzain activity was measured as previously described,[15b] by monitoring the cleavage of the fluorogenic substrate Z-Phe-Arg-aminomethylcoumarin (Z-FR-AMC). Assays were performed in a final volume of 200 μL, in sodium acetate 0.1 M pH 5.5, in the presence of 5 mM dithiothreitol and 0.01% Triton X-100, except for evaluation of detergent-sensitivity, when inhibition was compared in 0% and 0.01% Triton. Final concentrations were 0.4 nM for the enzyme and 2.5 μM for the substrate (K_m = 2 μM). All assays were performed in duplicates and followed for 5 min, and activity was calculated based on initial rates. All compounds were initially tested at 100 μM, after a 10 min pre-incubation with cruzain. Compounds which inhibited over 50% of cruzain activity at this concentration were further evaluated for time-dependence and detergent-sensitivity, and their dose–response curves were determined. For evaluation of time-dependence, percentages of enzyme inhibition by a compound with or without pre-incubation with enzyme for 10 min were compared. During the pre-incubation step cruzain and compound concentrations were 10-fold higher than in the final assay. Since compounds were observed to be time-dependent, consistently with a covalent mode of inhibition, all subsequent assays were performed with a 10 min pre-incubation. Dose–response curves were determined based on ten compounds concentrations, varying from 100 μM to 1.5 nM in fourfold dilutions and at 200 μM. Data was analyzed with Prism 4 (GraphPad). To evaluate if compounds were aggregators,[29] cruzain inhibition was compared for a given compound concentration in the absence of or in the presence of 0.01% Triton X-100. Compound concentrations varied depending on their potency against cruzain, and concentrations around their IC_{50}s were tested. Detergent-sensitivity was not observed.

5.2.2. Cytotoxicity screens

The cytotoxicity was determined using BALB/c mice splenocytes (5×10^6 cells $well^{-1}$) cultured in 96-well plates in Dulbecco's Mod-

ified Eagle's Medium (DMEM, Sigma Chemical Co., USA) supplemented with 10% of fetal calf serum (FCS; Cultilab, Brazil) and 50 μg mL^{-1} of gentamycin (Novafarma, Brazil). Each compound was evaluated in four concentrations (1, 5, 10 and 100 μg mL^{-1}), in triplicate. Cultures were incubated in the presence of ^{3}H-thymidine (1 μCi $well^{-1}$) for 24 h at 37 °C and 5% CO_2. After this period, the content of the plate was harvested to determine ^{3}H-thymidine incorporation using a beta-radiation counter (β-matrix 9600, Packard). The cytotoxicity of the compounds was determined by comparing the percentage of ^{3}H-thymidine incorporation (as an indicator of cell viability) of drug-treated wells in relation to untreated wells. Non-cytotoxic concentrations were defined as those causing a reduction of ^{3}H-thymidine incorporation below 10% in relation to untreated cells (control).

5.2.3. *T. cruzi* cell culture assay

Epimastigotes of *T. cruzi* (Y strain) were cultivated at 26 °C in Liver Infusion Tryptose medium supplemented with 10% fetal calf serum, 1% hemin, 1% R9 medium and 50 μg mL^{-1} gentamycin. Parasites (10^6 cells mL^{-1}) were cultured in a fresh medium in the absence or in the presence of the compounds being tested (from stock solution in DMSO). Cell growth was determined after 15 h, 7 and 11 days of culture by counting viable forms in a hemacytometer. The compounds were prepared from a stock solution in DMSO. To determine IC_{50}, cultures of Y strain epimastigotes in the presence of different concentrations of the compounds were evaluated after 11 days as described above. IC_{50} calculation was carried out using non-linear regression on Prism 4.0 GraphPad software. Y strain *T. cruzi* trypomastigotes were obtained from culture supernatants of the LCC-MK2 cell line at 37 °C and placed in 96-well plates (4×10^5 $well^{-1}$) in DMEM medium supplemented with 10% FCS and 50 μg mL^{-1} gentamycin. Tests were conducted in triplicate. Viable parasites were counted in a hemacytometer 24 h after addition of compounds by way of trypan blue exclusion. The percentage of inhibition was calculated in relation to untreated cultures. The same procedure was performed for Benznidazole (**Bdz**, reference drug) and vehicle alone, with DMSO blank.

5.2.4. Toxicological tests in mice

The selected compounds were re-suspended in 100 μL [30% DMSO/70% H_2O, v/v] and female Swiss mice weighting 40–45 g (n = 6 animals) were treated with a single dose of respective compounds (100 mg kg^{-1} weight). The treated animals were monitored for signs of general toxicity, including behavior and feeding, for 72 h after the last treatment. The number of dead animals was checked and compared with the untreated animals, which received 100 μL of solution (30% DMSO/70% H_2O, v/v). The experimental protocols with animals were approved and supervised by the Ethics Committee at the HEMOPE Hospital (Recife, PE, Brazil).

Acknowledgements

This research received support from Pernambuco State Foundation for Science and Technology (FACEPE, Grant #APQ-0123-4.03/08) and Brazilian National Council of Research (CNPq, Grant #472880/2009-8). M.V.O.C. holds a CAPES scholarship, while J.H.M. acknowledges the Sandler Family Foundation. We also thank the Federal University of Pernambuco Department of Fundamental Chemistry for recording the spectra and elemental analyses and HEMOPE Hospital for supplying mice for the toxicological test.

Supplementary data

CCDC 793133 (**3g**) contains the supplementary crystallographic data for this paper. These data can be obtained charge free from The Cambridge Crystallographic Data Centre via www.ccdc.cam.ac.uk/data_request/cif. Supplementary data (X-ray diffraction data for **3g** compound, HRMS and elemental analysis data of all new compounds) associated with this article can be found, in the online version, at doi:10.1016/j.bmc.2010.09.056.

References and notes

1. Coura, J. C. *Mem. Inst. Oswald Cruz.* **2007**, *112*, 113–122.
2. Cerecetto, H.; Gonzalez, M. *Curr. Top. Med. Chem.* **2002**, *2*, 1185–1211.
3. Hunter, W. N. *J. Biol. Chem.* **2009**, *284*, 11749–11753.
4. (a) Steverding, D.; Caffrey, C. R.; Sajid, M. *Mini-Rev. Med. Chem.* **2006**, *6*, 1025–1032; (b) Caffrey, C. R.; Steverding, D. *Mol. Biochem. Parasitol.* **2009**, *167*, 12–19.
5. (a) Ariyanayagam, M. R.; Oza, S. L.; Mehlert, A.; Fairlamb, A. H. *J. Biol. Chem.* **2003**, *278*, 27612–27619; (b) Eberle, C.; Burkhard, J. A.; Stump, B.; Kaiser, M.; Brun, R.; Krauth-Siegel, R. L.; Diederich, F. *ChemMedChem* **2009**, *4*, 2034–2044.
6. (a) Neres, J.; Bryce, R. A.; Douglas, K. T. *Drug Discovery Today* **2008**, *13*, 110–117; (b) Carvalho, I.; Andrade, P.; Campo, V. L.; Guedes, P. M. M.; Sesti-Costa, R.; Silva, J. S.; Schenkman, S.; Dedola, S.; Hille, L.; Rejzek, M.; Nepogodiev, S. A.; Field, R. A. *Bioorg. Med. Chem.* **2010**, *18*, 2412–2427.
7. (a) Santos, C. C.; Sant'Anna, C.; Terres, A.; Cunha-e-Silva, N. L.; Scharfstein, J.; Lima, A. P. C.; De, A. *J. Cell. Sci.* **2005**, *118*, 901–915; (b) Duschak, V. G.; Couto, A. S. *Curr. Med. Chem.* **2009**, *16*, 3174–3202.
8. (a) Scharfstein, J.; Schmitz, V.; Morandi, V.; Capella, M. M.; Lima, A. P.; Morrot, A.; Juliano, L.; Müller-Esterl, W. *J. Exp. Med.* **2000**, *192*, 1289–1300; (b) Aparicio, I. M.; Scharfstein, J.; Lima, A. P. C. A. *Infect. Immun.* **2004**, *72*, 5892–5902; (c) Acosta, D. M.; Arnaiz, M. R.; Esteva, M. I.; Barboza, M.; Stivale, D.; Orlando, U. D.; Torres, S.; Laucella, S. A.; Couto, A. S.; Duschak, V. G. *Int. Immunol.* **2008**, *20*, 461–470.
9. (a) Engel, J. C.; Doyle, P. S.; Hsieh, I.; McKerrow, J. H. *J. Exp. Med.* **1998**, *188*, 725–734; (b) Doyle, P. S.; Zhou, Y. M.; Engel, J. C.; McKerrow, J. H. *Antimicrob. Agents Chemother.* **2007**, *51*, 3932–3939.
10. Moreira, D. R. M.; Leite, A. C. L.; Santos, R. R.; Soares, M. B. P. *Curr. Drug Targets* **2009**, *10*, 212–231.
11. Du, X.; Hansell, E.; Engel, J. C.; Caffrey, C. R.; Cohen, F. E.; Mckerrow, J. H. *Chem. Biol.* **2000**, *7*, 733–742.
12. Du, X.; Guo, C.; Hansell, E.; Doyle, P. S.; Caffrey, C. R.; Holler, T. P.; McKerrow, J. H.; Cohen, F. E. *J. Med. Chem.* **2002**, *45*, 2695–2707.
13. Greenbaum, D. C.; Mackey, Z.; Hansell, E.; Doyle, P.; Gut, J.; Caffrey, C. R.; Lehrman, J.; Rosenthal, P. J.; McKerrow, J. H.; Chibale, K. *J. Med. Chem.* **2004**, *47*, 3212–3219.
14. (a) Fujii, N.; Mallari, J. P.; Hansell, E.; Mackey, Z.; Doyle, P.; Zhou, Y. M.; Gut, J.; Rosenthal, P. J.; McKerrow, J. H.; Guy, R. K. *Bioorg Med. Chem. Lett.* **2005**, *15*, 121–123; (b) Siles, R.; Chen, S.; Zhou, M.; Pinney, K. G.; Trawick, M. L. *Bioorg. Med. Chem. Lett.* **2006**, *16*, 4405–4409.
15. (a) Ferreira, R. S.; Bryant, C.; Ang, K. K. H.; McKerrow, J. H.; Shoichet, B. K.; Renslo, A. R. *J. Med. Chem.* **2009**, *52*, 5005–5008; (b) Jadhav, A.; Ferreira, R. S.; Klumpp, C.; Mott, B. T.; Austin, C. P.; Inglese, J.; Thomas, C. J.; Maloney, D. J.; Shoichet, B. K.; Simeonov, A. *J. Med. Chem.* **2010**, *53*, 37–51.
16. (a) Rodrigues, C. R.; Flaherty, T. F.; McKerrow, J. H.; Springer, C.; Cohen, F. E. *Bioorg. Med. Chem. Lett.* **2002**, *12*, 1537–1541; (b) Porcal, W.; Hernández, P.; Boiani, L.; Boiani, M.; Ferreira, A.; Chidichimo, A.; Cazzulo, J. J.; Olea-Azar, C.; González, M.; Cerecetto, H. *Bioorg. Med. Chem.* **2008**, *16*, 6995–7004; (c) Zanatta, N.; Amaral, S. S.; Santos, J. M.; de Mello, D. L.; Fernandes, L. D. S.; Bonacorso, H. G.; Martins, M. A. P.; Andricopulo, A. D.; Borchhardt, D. M. *Bioorg. Med. Chem.* **2008**, *16*, 10236–10243; (d) Trossini, G. H.; Malvezzi, A.; do Amaral, A. T.; Rangel-Yagui, C. O.; Izidoro, M. A.; Cezari, M. H.; Juliano, L.; Chin, C. M.; Menezes, C. M.; Ferreira, E. I. *J. Enzyme Inhib. Med. Chem.* **2010**, *25*, 62–67.
17. (a) Brak, K.; Doyle, P. S.; McKerrow, J. H.; Ellman, J. A. *J. Am. Chem. Soc.* **2008**, *130*, 6404; (b) Brak, K.; Kerr, I. D.; Barrett, K. T.; Fuchi, N.; Debnath, M.; Ang, K.; Engel, J. C.; McKerrow, J. H.; Doyle, P. S.; Brinen, L. S.; Ellman, J. A. *J. Med. Chem.* **2010**, *53*, 1763–1773; (c) Mott, B. T.; Ferreira, R. S.; Simeonov, A.; Jadhav, A.; Ang, K. K. H.; Leister, W.; Shen, M.; Silveira, J. T.; Doyle, P. S.; Arkin, M. R.; McKerrow, J. H.; Inglese, J.; Austin, C. P.; Thomas, C. J.; Shoichet, B. K.; Maloney, D. J. *J. Med. Chem.* **2010**, *53*, 52–60.
18. (a) Romeiro, N. C.; Aguirre, G.; Hernández, P.; González, M.; Cerecetto, H.; Aldana, I.; Pérez-Silanes, S.; Monge, A.; Barreiro, E. J.; Lima, L. M. *Bioorg. Med. Chem.* **2009**, *17*, 641–652; (b) Santos-Filho, J. M.; Leite, A. C. L.; Oliveira, B. G.; Moreira, D. R. M.; Lima, M. S.; Soares, M. B. P.; Leite, L. F. C. C. *Bioorg. Med. Chem.* **2009**, *17*, 6682–6691; (c) Vera-Divaio, M. A. F.; Freitas, A. C.; Castro, H. C.; Albuquerque, S.; Cabral, L. M.; Rodrigues, C. R.; Albuquerque, M. G.; Martins, R. C. A.; Henriques, M. G. O.; Dias, L. R. S. *Bioorg. Med. Chem.* **2009**, *17*, 295–302; (d) Merlino, A.; Benitez, D.; Chavez, S.; Cunha, J.; Hernández, P.; Tinoco, L. W.; Campillo, N. E.; Páez, J. A.; Cerecetto, H.; González, M. *Med. Chem. Commun.* **2010**, *1*, 216–228.
19. Bryant, C.; Kerr, I. D.; Debnath, M.; Ang, K. K. H.; Ratnam, J.; Ferreira, R. S.; Jaishankar, P.; Zhao, D.-M.; Arkin, M. R.; McKerrow, J. H.; Brinen, L. S.; Renslo, A. R. *Bioorg. Med. Chem. Lett.* **2009**, *19*, 6218–6221.
20. Borchhardt, D. M.; Mascarello, A.; Chiaradia, L. D.; Nunes, R. J.; Oliva, G.; Yunes, R. A.; Andricopulo, A. D. *J. Braz. Chem. Soc.* **2010**, *21*, 142–150.
21. Leite, A. C. L.; Lima, R. S.; Moreira, D. R. M.; Cardoso, M. V. O.; Brito, A. C. G.; Santos, L. M. F.; Hernandes, M. Z.; Kiperstok, A. C.; Lima, R. S.; Soares, M. B. P. *Bioorg. Med. Chem.* **2006**, *14*, 3749–3757.

22. Leite, A. C. L.; Moreira, D. R. M.; Cardoso, M. V. O.; Hernandes, M. Z.; Pereira, V. R. A.; Silva, R. O.; Kiperstok, A. C.; Lima, M. S.; Soares, M. B. P. *ChemMedChem* **2007**, *2*, 1339–1345.
23. Donnici, C. L.; Araújo, M. H.; Oliveira, H. S.; Moreira, D. R. M.; Pereira, V. R. A.; Souza, M. deA.; Castro, M. C. A. B. de; Leite, A. C. L. *Bioorg. Med. Chem.* **2009**, *17*, 5038–5043.
24. (a) Lima, L. M.; Barreiro, E. J. *Curr. Med. Chem.* **2005**, *12*, 23–49; (b) Viegas-Junior, C.; Danuello, A.; Bolzani, V.; Da, S.; Barreiro, E. J.; Fraga, C. A. M. *Curr. Med. Chem.* **2007**, *14*, 103–112; (c) Hernandes, M. Z.; Cavalcanti, S. M. T.; Moreira, D. R. M.; Azevedo, W. F., Jr.; Leite, A. C. L. *Curr. Drug Targets* **2010**, *11*, 303–314.
25. Pessoa, C.; Ferreira, P. M. P.; Lotufo, L. V. C.; Moraes, M. O. de; Cavalcanti, S. T. C.; Coelho, L. C. D.; Hernandes, M. Z.; Leite, A. C. L.; De Simone, C. A.; Costa, V. M. A.; Souza, V. M. O. *ChemMedChem* **2010**, *5*, 523–528.
26. (a) Leite, A. C. L.; Moreira, D. R. M.; Coelho, L. C. D.; Menezes, F. D. de; Brondani, D. J. *Tetrahedron Lett.* **2008**, *49*, 1538–1541; (b) Alves, A. J.; Leite, A. C. L.; Santana, D. P.; Beltrao, M. T.; Coelho, M. R.; Gayral, P. *Farmaco* **1993**, *48*, 1167–1171.
27. (a) Vicini, P.; Geronikaki, A.; Anastasia, K.; Incertia, M.; Zani, F. *Bioorg. Med. Chem.* **2006**, *14*, 3859–3863; (b) Vicini, P.; Geronikaki, A.; Incerti, M.; Zani, F.; Dearden, J.; Hewitt, M. *Bioorg. Med. Chem.* **2008**, *16*, 3714–3724; (c) Lopez-Torres, E.; Dilworth, J. R. *Chem. Eur. J.* **2009**, *15*, 3012–3023.
28. Ozturk, T.; Ertas, E.; Mert, O. *Chem. Rev.* **2007**, *107*, 5210–5278.
29. Seidler, J.; McGovern, S. L.; Doman, T. N.; Shoichet, B. K. *J. Med. Chem.* **2003**, *46*, 4477–4486.
30. Feng, B. Y.; Shoichet, B. K. *Nat. Protocols* **2006**, *1*, 550–553.
31. Rocha, G. B.; Freire, R. O.; Simas, A. M.; Stewart, J. J. P. *J. Comput. Chem.* **2006**, *27*, 1101–1111.
32. Spartan '08 Tutorial and User's Guide; Wavefunction: Irvine, CA, 2008. http://www.wavefun.com/products/spartan.html.
33. Choe, Y.; Brinen, L. S.; Price, M. S.; Engel, J. C.; Lange, M.; Grisostomi, C.; Weston, S. G.; Pallai, P. V.; Cheng, H.; Hardy, L. W.; Hartsough, D. S.; Mcmakin, M.; Tilton, R. F.; Baldino, C. M.; Craik, C. S. *Bioorg. Med. Chem.* **2005**, *13*, 2141–2156.
34. GOLD version 4.0 software, Cambridge Crystallographic Data Centre. http://www.ccdc.cam.ac.uk.
35. W.L. DeLano, The PyMOL Molecular Graphics System, DeLano Scientific: San Carlos, CA, USA, 2002. http://www.pymol.org.